EPJ Web of Conferences **319**, 04003 (2025) https://doi.org/10.1051/epjconf/202531904003
RICAP-24

Progressing our understanding of cosmic rays with the HERD space-borne experiment

Chiara Perrina[1,*] on behalf of the HERD Collaboration

[1]Institute of Physics, Ecole Polytechnique Fédérale de Lausanne (EPFL), CH-1015 Lausanne, Switzerland

Abstract. A new generation of space experiments is needed to enhance our understanding of cosmic rays. The challenge of the direct detection at ever higher energies, with improved energy and angular resolutions, is guiding us in the design of future detectors. The High Energy cosmic-Radiation Detection facility (HERD) onboard the China Space Station will be the next calorimetric experiment. Starting from 2027 and for more than 10 years, HERD will be measuring cosmic protons and heavier nuclei from 30 GeV/nucleon to a few PeV/nucleon. It will search for dark-matter signatures in the energy spectrum of cosmic electrons from 10 GeV to 100 TeV and photons from 100 MeV to 100 TeV. The HERD design, prospects and expected performance, as well as its role in multimessenger astronomy will be presented in this contribution.

1 Introduction

In recent years, experiments such as AMS (Alpha Magnetic Spectrometer) and DAMPE (DArk Matter Particle Explorer) have significantly advanced our understanding of cosmic rays (CRs). These missions have provided detailed measurements of cosmic-ray spectra, revealing intriguing and unexpected features that challenge the currently accepted supernova-remnant model [1]. For instance, AMS has measured, with unprecedented precision, a surplus of positrons at energies above 10 GeV, potentially pointing to dark-matter annihilation or astrophysical sources like pulsars. DAMPE, on the other hand, has detected a sharp drop in the electron + positron spectrum around 1 TeV. Despite these advances, critical questions remain. The exact mechanisms driving cosmic-ray acceleration in sources like supernova remnants are still poorly understood, as are the processes governing their propagation through the interstellar medium. Furthermore, while the nature of dark matter continues to elude detection both in underground experiments and in production searches at particle colliders, current cosmic-ray observations offer tantalizing yet inconclusive clues. The goal of HERD is to address these challenges with unprecedented acceptance and wide energy coverage, providing a clearer picture of these enigmatic phenomena.

2 HERD observables and objectives

Cosmic electrons and positrons: A major scientific goal of HERD is the measurement of the cosmic electron-plus-positron (CRE) spectrum up to 100 TeV. Investigating the CRE flux

*e-mail: Chiara.Perrina@epfl.ch

above 1 TeV is particularly significant, as electrons with energies above 100 GeV lose energy primarily through inverse Compton scattering and synchrotron radiation, which limits their propagation distance. Consequently, electrons above a few TeV are likely to originate from nearby sources (< 1 kpc) or from dark-matter annihilation and/or decay. As mentioned above, precision measurements from AMS [2] have confirmed a rise in the positron fraction between 8 GeV and 500 GeV, first observed with PAMELA [3]. This excess could be attributed to either astrophysical sources or dark-matter processes. The break in the CRE spectrum observed with DAMPE at 0.9 TeV [4] suggests a possible upper-energy limit for the cosmic electron spectrum [5]. In this scenario, the positron spectrum cutoff is expected below 0.9 TeV, as observed with AMS [6]. HERD will provide the high-resolution measurements needed to clarify the origin of the positron excess, distinguishing between contributions from local astrophysical sources and potential dark-matter signals. Fig. 1 illustrates the expected cosmic electron-plus-positron flux as measured with HERD over five years, accounting for contributions from nearby sources.

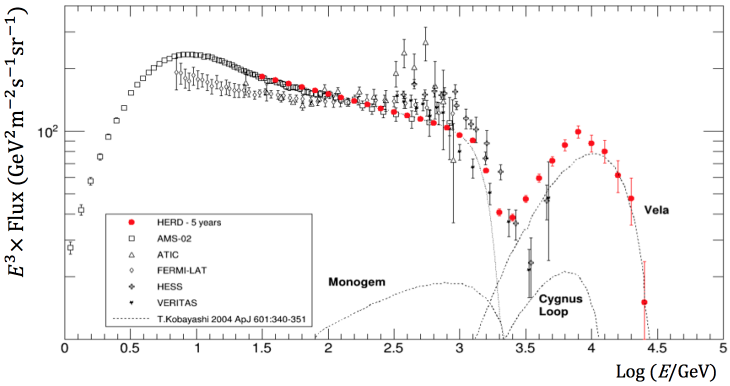

Figure 1: Simulated $e^- + e^+$ energy flux as measured with HERD over a five-year observation period. Measurements from other experiments are also shown for reference.

Cosmic protons and heavy nuclei: HERD will enable the measurement of the flux of protons and helium nuclei up to a few PeV, as well as heavier nuclei, including iron, up to several hundreds of TeV per nucleon. This will provide valuable insights into the production, acceleration and propagation mechanisms of cosmic rays. HERD will directly probe the "knee" of the all-particle flux, a region where ground-based experiments have observed a change in the spectral index, which may indicate the confinement limit of high-energy particles by the galactic magnetic field, along with the contribution from extragalactic sources. HERD will improve the measurements of secondary-to-primary flux ratios, such as boron-to-carbon (B/C) and boron-to-oxygen (B/O), which are crucial for studying the propagation of cosmic rays in the Galaxy. Although current measurements in the TeV-per-nucleon range are limited by low statistics, HERD will address this by providing more precise data, extending the measurement of CR energy spectra and mass composition up to a few PeV. Recent measurements have revealed unexpected spectral features below the knee. AMS has shown that the fluxes of protons, helium through neon, magnesium, silicon and iron nuclei [7, 8] deviate from a single power law, with a progressive hardening observed above 200 GV. DAMPE observed a softening in the proton flux around 14 TeV [9] and in the helium flux around 34 TeV [10]. HERD will further investigate these features and extend measurements to higher energies, directly exploring the knee structure. Fig. 2 illustrates the simulated energy spectra

for protons (left) and helium (center), as well as the boron-to-carbon flux ratio (right), based on five years of HERD data.

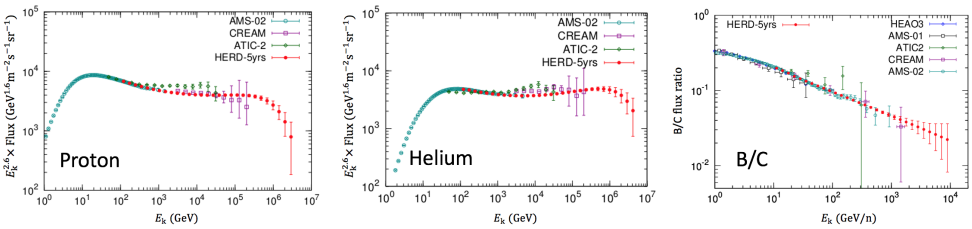

Figure 2: Simulated proton (left) and helium (center) energy spectra and boron-to-carbon flux ratio (right) as measured with HERD over a five-year observation period. Measurements from other experiments are also shown for reference.

Cosmic gamma rays: Due to its large acceptance and sensitivity, HERD will conduct a comprehensive gamma-ray survey of the full sky for energies above 100 MeV. This will enable the study of both galactic and extragalactic gamma-ray point sources, diffuse emissions and transient phenomena. In the era of multimessenger and multiwavelength astronomy, monitoring the gamma-ray sky from space remains crucial. The importance of such efforts was demonstrated by the Fermi-LAT detection of the electromagnetic counterpart to a binary neutron star merger observed with LIGO/Virgo [11]. With its exceptionally large field of view and broad energy range, HERD will play a pivotal role in multiwavelength studies across the electromagnetic spectrum, complementing other telescopes operating in radio, optical, X-ray and gamma-ray bands. HERD will also search for electromagnetic counterparts of gravitational-wave events detected with LIGO [12], Virgo [13], KAGRA [14] and GEO [15], as well as neutrino events observed with IceCube [16] and KM3NeT [17]. Additionally, HERD will provide alerts for transient events. The expected sky map produced with HERD after five years of operation is shown in Fig. 3. One of the main HERD objectives is the search for dark-matter signatures in the gamma-ray spectrum. Signals from two-body dark-matter annihilation or dark-matter decay could manifest as a sharp peak over the diffuse gamma-ray background. HERD will search for such gamma-ray lines in the energy range from 10 GeV to 100 TeV, achieving unprecedented sensitivity.

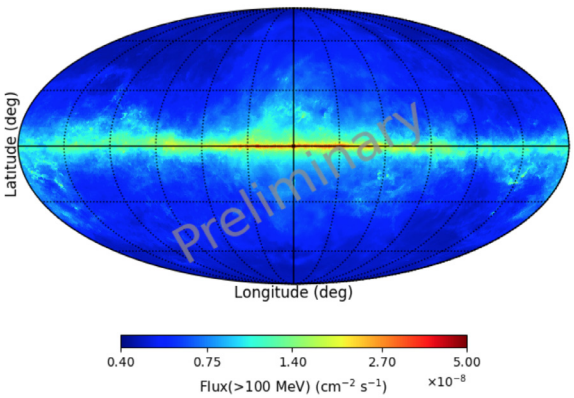

Figure 3: Simulated gamma-ray sky map in galactic coordinates, based on HERD measurements over a five-year observation period [18].

3 The HERD detector

To explore energies never before reached in space, HERD has been designed with a calorimeter of unprecedented depth, surrounded by a nearly isotropic configuration. An exploded view of the detector is presented in Fig. 4. Specifically, the calorimeter (CALO) is enclosed on the

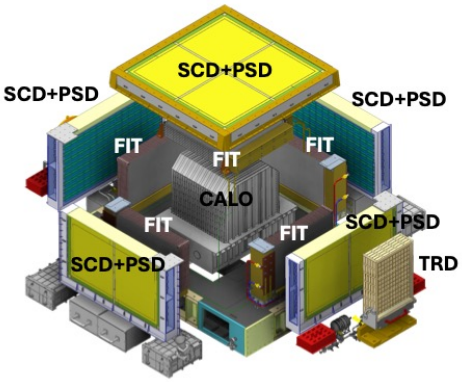

Figure 4: Exploded view of the HERD experiment. The core detector is the calorimeter (CALO), surrounded on the top and four lateral sides by a sector of the scintillating-fiber tracker (FIT), the plastic scintillator detector (PSD) and the silicon charge detector (SCD). The transition radiation detector (TRD) is mounted on one of the lateral sides.

top and four lateral sides by the scintillating-fiber tracker (FIT), the plastic scintillator detector (PSD) and the silicon charge detector (SCD), with a transition radiation detector (TRD) placed on one of the lateral sides. Thanks to this innovative design, HERD offers a geometric acceptance approximately ten times larger than that of current-generation detectors. The detector has been optimized to minimize systematic uncertainties, especially regarding the absolute energy scale. For this purpose, TRD is used to calibrate the response of the calorimeter to high-energy hadronic showers and CALO is read out with two independent systems. SCD, located at the outermost detector, measures the particle charge before any possible nuclear fragmentation. The expected performance of HERD, including angular, charge and energy resolutions, electron/proton separation power and geometric acceptance, is summarized in Table 1.

Table 1: Expected HERD performance

Angular resolution (e, γ)	0.1° at 10 GeV
Charge resolution (nuclei)	10% - 15% for $Z = 1 - 26$
Energy resolution (e, γ)	$< 1\%$ at 100 GeV
Energy resolution (p)	20% at 100 GeV – PeV
e/p separation power	$> 10^6$
Geometric factor (e)	> 3 m^{2}sr at 200 GeV
Geometric factor (p)	> 2 m^{2}sr at 100 GeV

CALO [19] is a 3D, homogeneous, isotropic and finely segmented calorimeter. It consists of approximately 7500 LYSO crystals, each with a 3 cm edge, arranged in a nearly spherical configuration. The total depth of CALO is about 55 radiation lengths and 3 nuclear interaction lengths. The scintillation light induced by charged particles passing through the crystals is detected with two independent read-out systems. One system uses wavelength-shifting fibers (WLS) coupled with image-intensified scientific CMOS (IsCMOS) cameras,

while the other employs photodiodes connected to custom front-end electronics chips, named HIDRA. This dual read-out system provides redundancy and independent triggering, enables the cross calibration, thus minimizing systematic uncertainties. The performance of a CALO prototype, evaluated at the CERN SPS with electron beams, is shown in Fig. 5. The left panel displays the distribution of the energy deposited by 100 GeV electrons, as measured with the photodiode system. A fit with a logarithmic Gaussian function is performed to estimate the peak position. The standard deviation is computed as half the width of the energy interval centered around the peak that contains 68% of the events. The energy resolution, defined as the ratio of the standard deviation to the peak position, is shown in the right panel as a function of the electron beam energy.

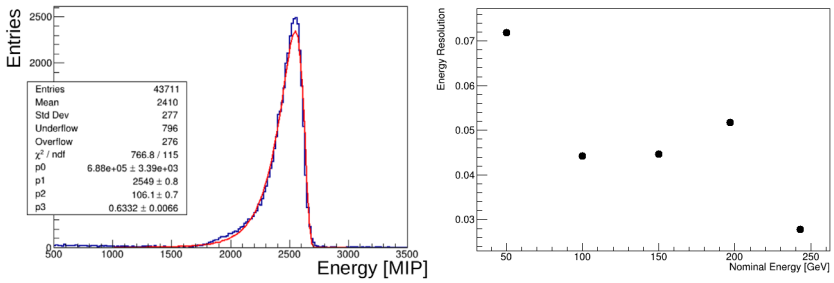

Figure 5: Distribution of deposited energy for 100 GeV electrons, fitted with a logarithmic Gaussian function (left). Energy resolution as a function of electron energy (right) [19].

FIT [20, 21] is designed to reconstruct the trajectory of charged particles passing through the detector. In addition, FIT provides a redundant measurement of the absolute value of the particle electric charge ($|Z|$) and enables the detection of low-energy gamma rays ($>$ 100 MeV) enhancing their conversion into electron-positron pairs. FIT consists of five tracking sectors, each made up of seven tracking planes. Each plane consists of two layers of FIT modules measuring the two orthogonal spatial coordinates. A FIT module is made of a scintillating-fiber mat and a front-end board that contains three linear arrays, each with 128 silicon photomultipliers (SiPMs). The scintillating-fiber mat is composed of six layers of fibers produced by Kuraray (type SCSF-78MJ), each with a round cross section and an average diameter of 250 μm. The mat has a width of 97.8 mm, which aligns with three Hamamatsu S13552-10 SiPM arrays. The front-end board also contains six BETA-64 ASICs [22]. These custom designed ASICs provide single-photon resolution with dual-path automatic gain switching, ensuring a high dynamic range without saturation, even when all SiPM pixels are activated. Additionally, they operate within a low-power budget, consuming less than 1 mW per channel. To demonstrate the tracking and charge measurement capabilities of FIT and the first version of the BETA-16 ASIC, a miniature of the top FIT sector called MiniFIT [23] was designed, produced, and tested using a secondary-ion beam at the CERN SPS. The left panel of Fig. 6 shows the charge distribution for the reconstructed nuclei (beam composition), fitted with a multi-Gaussian function. The Gaussian peaks correspond to different nuclear species. The center panel of Fig. 6 presents the measured mean charge as a function of the nuclear charge. Ongoing studies focus on correcting the deviation from the expected linear relationship. These studies take into account saturation effects in both the SiPMs and the scintillating fibers and will extend the track and charge reconstruction to heavier nuclei. The right panel of Fig. 6 shows the distribution of track-hit residuals on an internal tracking layer for reconstructed carbon ($Z = 6$) tracks, fitted with a Gaussian function. The measured position resolution for carbon nuclei with normal incidence is 25 μm.

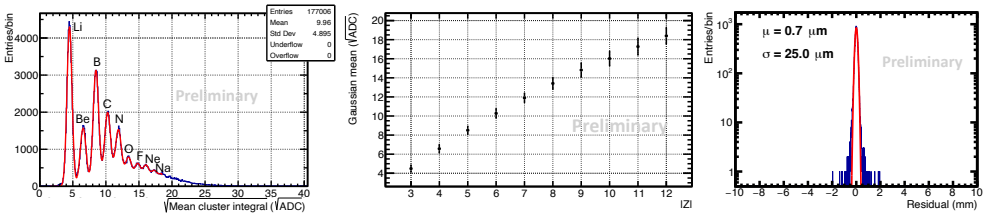

Figure 6: Charge distribution for the reconstructed nuclei, with Gaussian peaks corresponding to the identified nuclear species (left). Measured mean charge as a function of nuclear charge (center). Distribution of track-hit residuals on an internal MiniFIT layer for carbon nuclei, fitted with a Gaussian function (right) [23].

PSD [24] will be used to efficiently distinguish photons from charged particles and measure the charge of the latter up to $Z = 26$. The five faces of PSD surround the five FIT sectors. Its design is being optimized to achieve high detection efficiency for charged particles (> 99.98%), a broad dynamic range for identifying nuclei up to iron, and good segmentation to minimize the pile-up effect caused by secondary particles back scattered from the calorimeter. The proposed configuration consists of trapezoidal scintillator tiles read out with SiPMs. A prototype detector, consisting of eight trapezoidal plastic-scintillator bars of two distinct lengths, each equipped with SiPMs positioned at different locations along the bars, was tested using a secondary-ion beam at the CERN SPS. The left-hand plot in Fig. 7 shows the overall signal distribution, along with the signal distributions for the various nuclei. The right-hand plot in Fig. 7 displays the mean signal as a function of the squared nuclear charge, with the red curve representing the best-fit line derived from Birks' law.

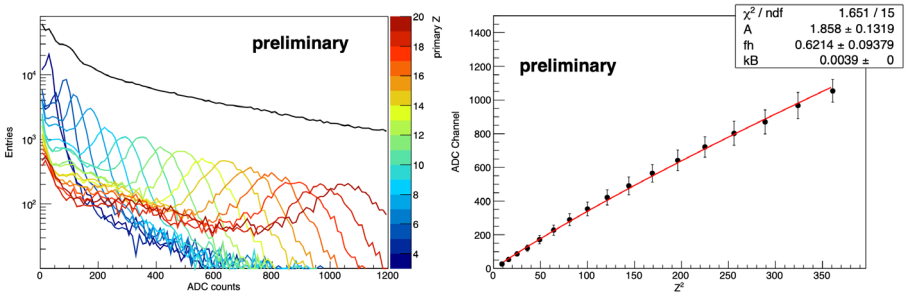

Figure 7: Overall signal distribution, along with signal distributions for individual nuclei (left). Mean signal as a function of the squared nuclear charge, the red curve represents the best-fit line derived from Birks' law (right) [24].

SCD [25] is designed to accurately measure the absolute electric charge of cosmic nuclei, enabling the separation of chemical species from hydrogen to iron and beyond. It consists of four x-y layers of single-sided silicon micro-strip detectors (SSDs), providing eight independent ionization energy loss measurements per sector. As the outermost detector, SCD will measure the particle charge before any early charge-change interactions occur in PSD. The strip pitch and the distance between SCD and PSD are designed to minimize the pile-up effect caused by the back-scattered secondary particles from CALO. The eight-layer configuration is optimized for precise charge measurements and has been validated through Monte Carlo simulations. Each SSD measures 95×95 mm^2. The total sensitive area of SCD is approximately 60 m^2. Fig. 8 shows the charge distribution for SSDs with 60 μm strip width and 20 pF

capacitance, tested using a secondary-ion beam at the CERN SPS. The results demonstrate the SCD charge separation capability up to at least $Z = 28$.

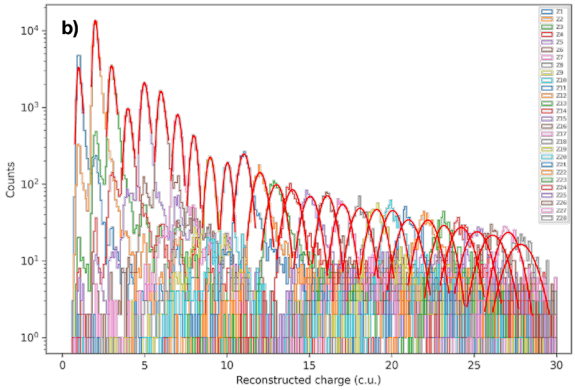

Figure 8: Charge distribution for the reconstructed nuclei, with Gaussian peaks corresponding to the identified nuclear species [25].

TRD [26] will be used to calibrate the response of the calorimeter to high-energy hadronic showers. CALO calibration is currently performed at CERN, using particle beams with known energy, up to a few hundred GeV. TRD will allow this calibration to higher energies. To date, CREAM [27] is the only experiment that has performed an in-flight cross calibration between a calorimeter and a transition-radiation detector. The TRD response depends on the particle gamma factor, and the gamma factor of electrons between 0.5 GeV and 5 GeV is equivalent to that of protons between 1 TeV and 10 TeV. Therefore, the calibration procedure consists of two steps: first, the TRD response is calibrated on ground using electron beams with energies from 0.5 GeV to 5 GeV; then, the CALO response will be calibrated in flight using identified protons with energies between 1 TeV and 10 TeV. To isolate the TR signal from the ionization energy loss background, the detector is designed with a modular structure, incorporating a TR radiator and a thick gaseous electron multiplier (THGEM) with an effective area of $20 \times 20\,\mathrm{cm}^2$. The top panel of Fig. 9 shows the energy spectra measured with a TRD prototype for two different electron momenta. The simulated individual contributions to the total energy spectra (ionization energy loss and TR), as well as their sum, are also shown. The bottom panel illustrates the deviation between the measured and simulated spectra within each energy bin. The excellent agreement between Monte Carlo simulations and experimental data highlights the accuracy of the implemented models.

4 Conclusions

HERD will be the next experiment for the direct detection of cosmic and gamma rays. Its primary scientific objectives include the indirect detection of dark matter through precise measurements of the electron + positron and gamma-ray spectra, exploring potential signatures of exotic physics. Furthermore, HERD will monitor gamma rays across the entire sky, shedding light on the most energetic phenomena in the Universe. By detecting cosmic electrons, positrons, protons, and heavier nuclei with unprecedented accuracy, HERD will progress our understanding of the origin, acceleration and propagation of cosmic particles. This will pave the way for new discoveries in fundamental physics and astrophysics.

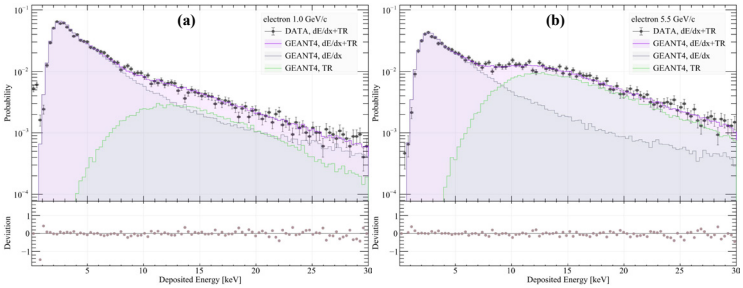

Figure 9: Simulated and measured transition-radiation and ionization energy spectra for 1.0 GeV/c electrons (left) and 5.5 GeV/c electrons (right). The bottom panels show the deviation between data and simulations [26].

Acknowledgments

The author gratefully acknowledges the financial support from the Swiss National Science Foundation (SNSF-PZ00P2_193523).

References

[1] S. Gabici et al., Int. J. Mod. Phys. D **28**, 1930022 (2019). 10.1142/S0218271819300222
[2] AMS Collaboration, Phys. Rev. Lett. **113**, 121101 (2014). 10.1103/PhysRevLett.113.121101
[3] PAMELA Collaboration, Nature **458**, 607 (2009). 10.1038/nature07942
[4] DAMPE Collaboration, Nature **552**, 63 (2017). 10.1038/nature24475
[5] K. Fang et al., ApJ **854**, 57 (2018). 10.3847/1538-4357/aaa710
[6] AMS Collaboration, Phys. Rev. Lett. **122**, 041102 (2019). 10.1103/PhysRevLett.122.041102
[7] AMS Collaboration, Physics Reports **894**, 1 (2021). 10.1016/j.physrep.2020.09.003
[8] J. Berdugo, Moscow University Physics Bulletin **77**, 71 (2022). 10.3103/S0027134922020126
[9] DAMPE Collaboration, Sci. Adv. **5**, eaax3793 (2019). 10.1126/sciadv.aax3793
[10] DAMPE Collaboration, Phys. Rev. Lett. **126**, 201102 (2021). 10.1103/PhysRevLett.126.201102
[11] Fermi-LAT Collaboration, ApJ **861**, 85 (2018). 10.3847/1538-4357/aac515
[12] LIGO Scientific Collaboration, Class. Quantum Grav. **32**, 074001 (2015). 10.1088/0264-9381/32/7/074001
[13] Virgo Collaboration, Class. Quantum Grav. **32**, 024001 (2015). 10.1088/0264-9381/32/2/024001
[14] KAGRA Collaboration, Galaxies **10**, 63 (2022). 10.3390/galaxies10030063
[15] K.L. Dooley et al., Class. Quantum Grav. **33**, 075009 (2016). 10.1088/0264-9381/33/7/075009
[16] M. Ahlers et al., Eur. Phys. J. C **78**, 924 (2018). 10.1140/epjc/s10052-018-6369-9
[17] KM3NeT Collaboration, J. Phys. G: Nucl. Part. Phys. **43**, 084001 (2016). 10.1088/0954-3899/43/8/084001
[18] L. Fariña et al., PoS **ICRC2021**, 651 (2021). 10.22323/1.395.0651
[19] P. Betti et al., Instruments **8** (2024). 10.3390/instruments8010005
[20] C. Perrina et al., PoS **ICRC2021**, 067 (2021). 10.22323/1.395.0067
[21] J.J. Wang et al., Rad. Det. Tech. Meth. **5**, 389 (2021). 10.1007/s41605-021-00262-9
[22] S. Anand et al., Nuclear Science and Techniques **35**, 59 (2024). 10.1007/s41365-024-01419-z
[23] C. Perrina, PoS **ICHEP2024**, 694 (2024). 10.22323/1.476.0694
[24] D. Serini et al., PoS **ICRC2023**, 112 (2023). 10.22323/1.444.0112
[25] A. Oliva et al., PoS **ICRC2023**, 087 (2023). 10.22323/1.444.0087
[26] C. Dai et al., PoS **ICRC2023**, 113 (2023). 10.22323/1.444.0113
[27] P. Maestro et al., Proc. of the 30th ICRC **2**, 333 (2008). 10.48550/arXiv.1003.5753